Microchemical Journal 159 (2020) 105561

Contents lists available at ScienceDirect

Microchemical Journal

journal homepage: www.elsevier.com/locate/microc

Deltamethrin determination in natural water samples via photochemically-induced fluorescence coupled to third-order multivariate calibration

Rodrigo I. Veneciano [a], V. Sonnia Parra [a], Waldo Quiroz [a], Edwar Fuentes [b], Luis F. Aguilar [c], Manuel A. Bravo [a,*]

[a] Laboratorio de Química Analítica y Ambiental, Instituto de Química, Facultad de ciencias, Pontificia Universidad Católica de Valparaíso, Avenida Brasil 2950, Valparaíso, Chile
[b] Departamento de Química Inorgánica y Analítica, Facultad de Ciencias Químicas y Farmacéuticas, Universidad de Chile, Santiago, Casilla 233, Chile
[c] Laboratorio de Fotofísica y Espectroscopía Molecular, Instituto de Química, Facultad de ciencias, Pontificia Universidad Católica de Valparaíso, Avenida Brasil, 2950 Valparaíso, Chile

ARTICLE INFO

Keywords:
Photo-induced fluorescence
Multivariate calibration
Pyrethroids

ABSTRACT

In this work, an analytical method for deltamethrin determination in natural waters based on photochemically-induced fluorescence coupled to third-order/four-way calibration was evaluated and compared with second-order/three-way calibration. The four-way data were obtained during the photodegradation of deltamethrin in the form of excitation-emission fluorescence matrices and modelled by unfolded partial least squares coupled to residual trilinearization (U-PLS-RTL). According to the results, the third-order model resulted in a satisfactory fit and better figures of merit, even in the presence of unexpected interferences due to the additional dimension. In this way, the method presents a limit of detection of 2.9 μg L^{-1} and a relative error of prediction of 15.8%. The optimization of a dispersive liquid-liquid microextraction (DLLME) procedure reached an enrichment factor (EF) of 5, improving the detection and quantification limits. Finally, the analytical method based on third-order multivariate calibration was applied to quantify this analyte in spiked natural water samples, both directly and after preconcentration. In all cases, the third-order property allowed us to satisfactorily model the data and quantify this compound in these complex matrices, demonstrating the superior analytical performance of the high-order data evaluated.

1. Introduction

Pyrethroids are synthetic insecticides based on pyrethrins, which are natural insecticides present in chrysanthemums [1], and they are used worldwide due their high effectiveness and relatively low toxicity in comparison with other pesticides. However, pyrethroids have also shown toxic effects on aquatic organisms and can bioaccumulate, causing long-term adverse effects in aquatic environments [2]. In humans, exposure to pyrethroids can cause chronic diseases and have toxic effects on the nervous, immune, and cardiovascular systems as well as on genes, inducing teratogenic, carcinogenic and mutagenic effects [3,4]. Some studies have shown that pyrethroids could also affect male reproductive function [5]. Thus, sensitive and selective techniques are needed to monitor the presence of pyrethroids in different environmental compartments.

In general, the determination of pyrethroids is often based on laborious sample extraction procedures followed by chromatographic separation coupled to selective detection. Several extraction procedures have been developed, but the most common are based on liquid-liquid extraction (LLE) or solid-phase extraction (SPE) [6,7]. For the determination of pyrethroids, gas chromatography (GC) with electron capture (ECD) or mass spectrometry (MS) detection [8–10] has been preferably used, while liquid chromatography has been less common [11]. However, all of these methodologies are time consuming, require large volumes of organic solvent and produce large amounts of toxic organic solvent waste.

Fluorescence spectroscopy is an interesting alternative for the quantification of organic pollutants, showing high sensitivity,

* Corresponding author.
E-mail address: manuel.bravo@pucv.cl (M.A. Bravo).

https://doi.org/10.1016/j.microc.2020.105561
Received 27 July 2020; Received in revised form 19 September 2020; Accepted 19 September 2020
Available online 28 September 2020

selectivity, simplicity and low cost. Pyrethroid insecticides have no native fluorescence but can be (photo)chemically degraded, resulting in fluorescent photoproducts [12]. This approach, termed photo-induced fluorescence (PIF), has been proposed for the determination of organophosphorus insecticides and pyrethroids, such as chlorpyriphos and deltamethrin, respectively, in different environmental samples [13–15]. Unfortunately, fluorescence spectroscopy is not a problem-free approach and can suffer from low selectivity for the analysis of complex samples. For this reason, the coupling of this spectroscopic technique with modern chemometric tools, such as multivariate calibration, offers a powerful alternative for the determination of various chemicals. This approach has been used to satisfactorily determine pesticides [16,17], agrochemicals [18], and pharmaceuticals [19] in different biological and environmental matrices. In accordance with the modelled data type, different calibration strategies can be proposed, where the second-order/three-way calibration allows the analyte information (e.g., analyte concentration) to be obtained from an unselective instrumental signal (e.g., analyte signal overlapped with the responses of unexpected interferences), a property known as a second-order advantage [20]. However, in the presence of extensive analyte overlap or sample-matrix effects during complex sample analysis, the second-order advantage cannot be attained, and an additional data dimension is required [21]. The satisfactory results obtained with third-order calibration to address serious collinearity problems between an analyte and interferences during complex sample analysis suggest that third-order/four-way calibration offers better modelling and predictions [22–24], although there is still no consensus about the existence of a "third-order advantage".

In this work, an analytical method for deltamethrin determination in natural waters is proposed. This method is based on photodegradation of this pyrethroid followed by total fluorescence spectroscopy and modelling by third-order multivariate calibration. Similar analytical methods have been evaluated for the determination of polycyclic aromatic hydrocarbons (PAHs) [25], fluoroquinolones [21] and neonicotinoid insecticides [26] in different matrices with satisfactory results. However, the evaluation of this approach for pyrethroid determination in environmental samples has been rare or is non-existent. First, the conditions for photodegradation were optimized, and the performances of different multivariate algorithms were evaluated. Then, the figures of merit were evaluated. Finally, this method was tested by analysing synthetic solutions containing unexpected interferences and different spiked natural water samples.

2. Theory of U-PLS-RBL and U-PLS-RTL

The principle of the U-PLS algorithm coupled to residual bilinearization (RBL) to achieve the second-order advantage has been previously reported for modelling three-way data [27]. In this method, the original second-order data are unfolded into vectors (JK × 1 size) by concatenating the original two-dimensional information vectors before first-order PLS is applied, as described by Wold et al. [28]. If no unexpected interferences are present in the test sample data, the regression coefficients $\boldsymbol{\nu}$ (size A × 1) can be employed to estimate the analyte concentration according to Eq. (1).

$$y_u = \mathbf{t}_u^T \boldsymbol{\nu} \tag{1}$$

where $\mathbf{t}_u$ (size A × 1) is the test sample score, obtained by projection of the unfolded data for test sample $\mathbf{X}_u$ [vec($\mathbf{X}_u$), size JK × 1] onto the space of the A latent factors. When unexpected constituents are detected in unknown sample $\mathbf{X}_u$, the PLS scores ($\mathbf{t}_u$) obtained are unsuitable for analyte prediction, and the residuals of the test sample signal (s_p) are significant. In this case, the residual contained in matrix $\mathbf{E}_p$ (see below) is abnormally large in comparison with the typical instrumental noise level. This phenomenon can be represented by Eq. (2).

$$s_p = \frac{\mathrm{vec}(\mathbf{E}_p)}{(JK - A)^{1/2}} = \frac{\mathrm{vec}(\mathbf{X}_u - P t_u)}{(JK - A)^{1/2}} \tag{2}$$

where $||\cdot||$ indicates the Euclidean norm, $\mathbf{P}$ is the matrix of loadings, vec $(\cdot)$ is the vectorization command, J and K are the number of instrumental channels in each data mode, and A corresponds to the number of PLS latent variables. To handle the presence of unexpected constituents, RBL resorts to principal component analysis (PCA) of the contribution from the unexpected components by minimizing the residuals $||e_u||$ computed using a Gauss-Newton procedure [27]. For a single unexpected component, the expression is

$$\mathrm{vec}(\mathbf{X}_u) = P t_u + \mathrm{vec}\left[g_{\mathrm{unx}} b_{\mathrm{unx}} (c_{\mathrm{unx}})^T\right] + e_u \tag{3}$$

where $\mathbf{b}_{\mathrm{unx}}$ and $\mathbf{c}_{\mathrm{unx}}$ are the left and right eigenvectors of $\mathbf{E}_p$ and g_{unx} is a scaling factor. The standard deviation (S_{RBL}) of the residuals in Eq. (3) can be used as a measure of the goodness of fit (GOF) for the RBL procedure. According to Bortolato et al. [29], S_{RBL} is given by Eq. (4).

$$s_{\mathrm{RBL}} = ||e_{\mathrm{RBL}}||/[(J - N_{\mathrm{unx}})(K - N_{\mathrm{unx}}) - A]^{1/2} \tag{4}$$

where N_{UNX} is the number of unexpected components. N_{UNX} is usually estimated by inspecting the behaviour of S_{RBL} with increasing N_{UNX}. The value of S_{RBL} is stabilized at the instrumental noise level when the correct value of N_{UNX} is reached.

For four-way calibration, U-PLS combined with residual trilinearization (RTL) constitutes an extension of U-PLS-RBL by one further dimension [30]. In this case, the third-order data ($\boldsymbol{X}_{JKL}$) are unfolded into vectors (JKL × 1 size), first-order PLS models are built, and the analyte concentration is estimated for a model similar to that in Eq. (1). If unexpected components are present in the sample ($\mathbf{X}_u$), they can be addressed by the RTL procedure based on a Tucker3 decomposition that models the interferents, minimizing the norm of the residual vector $\mathbf{e}_u$, which is computed while the sample data are fit to the sum of the relevant contributions to the sample signal [31]. For a single interferent, the relevant expression is Eq. (5).

$$\mathrm{vec}(\mathbf{X}_u) = \mathbf{P}\mathbf{t}_u + g_{\mathrm{int}}(\mathbf{d}_{\mathrm{int}} \otimes \mathbf{c}_{\mathrm{int}} \otimes \mathbf{b}_{\mathrm{int}}) + \mathbf{e}_u \tag{5}$$

where $\mathbf{b}_{\mathrm{int}}$, $\mathbf{c}_{\mathrm{int}}$ and $\mathbf{d}_{\mathrm{int}}$ are normalized profiles in the three modes for the interference and g_{int} is the first core element obtained by Tucker3 analysis of E_p as Eq. (6).

$$(g_{\mathrm{int}}, \mathbf{b}_{\mathrm{int}}, \mathbf{c}_{\mathrm{int}}, \mathbf{d}_{\mathrm{int}}) = \mathrm{Tucker3}(E_p) \tag{6}$$

The number of interferents N_i can be assessed by comparing the final residuals S_U with the instrumental noise level, with S_U given by Eq. (7).

$$S_u = \frac{\|\mathbf{e}_u\|}{[JKL - (N_C - N_i)]^{1/2}} \tag{7}$$

where e_u is the error presented in Eq. (5) and N_C is the number of calibrated components. Then, the RTL components (equivalent to the N_i components) are varied until S_U stabilizes at a value compatible with the experimental noise, allowing the correct number of components to be selected.

3. Experimental

3.1. Chemical and solvents

All the materials used in this study were analytical grade. Acetonitrile, hexane, dichloromethane and methanol were HPLC grade and were purchased from Merck (Darmstadt, Germany). Hydrogen peroxide was obtained from Merck (Darmstadt, Germany).

Sodium dodecyl sulphate surfactants (SDS) were purchased from Sigma-Aldrich (Steinheim, Germany), while hexadecyltrimethylammonium bromide (CTAB) was purchased from Loba Chemie

(Mumbai, India).

Standards of deltamethrin, imidacloprid and fipronil were purchased from Sigma-Aldrich (Steinheim, Germany). A concentrated solution was prepared by dissolving 1.0 mg of deltamethrin in 5.0 mL of methanol. The solution was stored in the dark at 8 °C for up to two weeks, during which it was shown to be stable. For daily work, a diluted solution of deltamethrin was prepared by diluting an adequate amount of the concentrated solution in 5.0 mL of methanol. A similar procedure was followed to prepare solutions of imidacloprid and fipronil.

Ultrapure water, obtained from a Milli-Q water purification system from Millipore (Bedford, MA, USA), was used in all work.

3.2. Instruments and software

An Agilent Cary-Eclipse fluorescence spectrometer (Santa Clara, CA, USA) equipped with a xenon flash lamp was used to obtain the excitation and emission matrices. The quartz cell had a sample volume of 700 µL and a path length of 1.00 cm and was obtained from Starna Scientific Ltd. (Hainault, Essex, United Kingdom). The excitation and emission slits were fixed at 10 nm. For the photodegradation studies, a UV-C mercury lamp obtained from Cole-Palmer (Vernon Hills, IL, USA) was used.

For the generation of four-way data for each sample to be analysed (calibration, validation and real samples), 0.5 mL of solution was added into a quartz cell and exposed to a UV-C lamp for photodegradation every minute from 0 to 4 min. For each exposure, the emission-excitation fluorescence matrices (EEFMs) were recorded every 3 nm over the λ_{EXC} range of 260–380 nm and every 2 nm over the λ_{EM} range of 290–450 nm. Thus, one EEFM was recorded at each photodegradation time point, and the dimension of the four-way data per sample was 81 × 41 × 5 (emission × excitation × time). Then, the EEFMs were saved in ASCII format and transferred to a computer for later manipulation. First, Rayleigh and Raman scattering signals were corrected using previously reported routines written in MATLAB [32]. Then, multivariate analysis was carried out using MATLAB 2012a. The MVC2 graphical interface was used for three-way data analysis [33], and the MVC3 graphical interface for four-way data analysis [34]. Both graphical interfaces allowed us to obtain different figures of merit, such as detection and quantification limits and sensitivity, among others.

3.3. Calibration and validation

For calibration, eight standard solutions of deltamethrin were prepared over a concentration range of 0–250 µg L^{-1} by diluting aliquots of a 5.0 mg L^{-1} standard. Adequate volumes of surfactant and hydroxide peroxide were added to obtain final concentrations of 11.0 mM and 5.0 mM, respectively. Finally, the EEFMs were registered and pre-processed according to the procedure described in the previous section (see Section 3.2), and the data were subjected to third- or second-order data analysis.

For validation, eight solutions were prepared containing deltamethrin, imidacloprid and fipronil over a concentration range of 0–200 µg L^{-1}, in accordance with a central composite design. In all solutions, the same concentrations of surfactant (SDS) and hydrogen peroxide as those in the calibration were used. Finally, each solution was exposed to a UV-C lamp for photodegradation followed by EEFM registration (see Section 3.2).

3.4. Analysis of real water samples

Different natural water samples were collected for this study: from La Luz dam placed in Valparaíso city, Chile (33°08′28.8″S 71°34′32.9″W); from an irrigation ditch in Villa Alemana city, Chile (33°02′14.6″S 71°22′53.1″W); and from well water in Casablanca city, Chile (33°18′39.3″S 71°25′10.0″W). Samples were collected in amber glass bottles and immediately transported to the laboratory, where the samples were filtered under vacuum through a nylon membrane (0.45 µm) and stored in amber glass flasks at −4°C until analysis. For direct analysis of these samples, 2.00 mL of a water sample was transferred into a 5.0 mL flask. Then, the solutions of surfactant and hydrogen peroxide were added to obtain final concentrations of 11 mM and 5 mM, respectively. The final volume was adjusted to 5.00 mL with methanol.

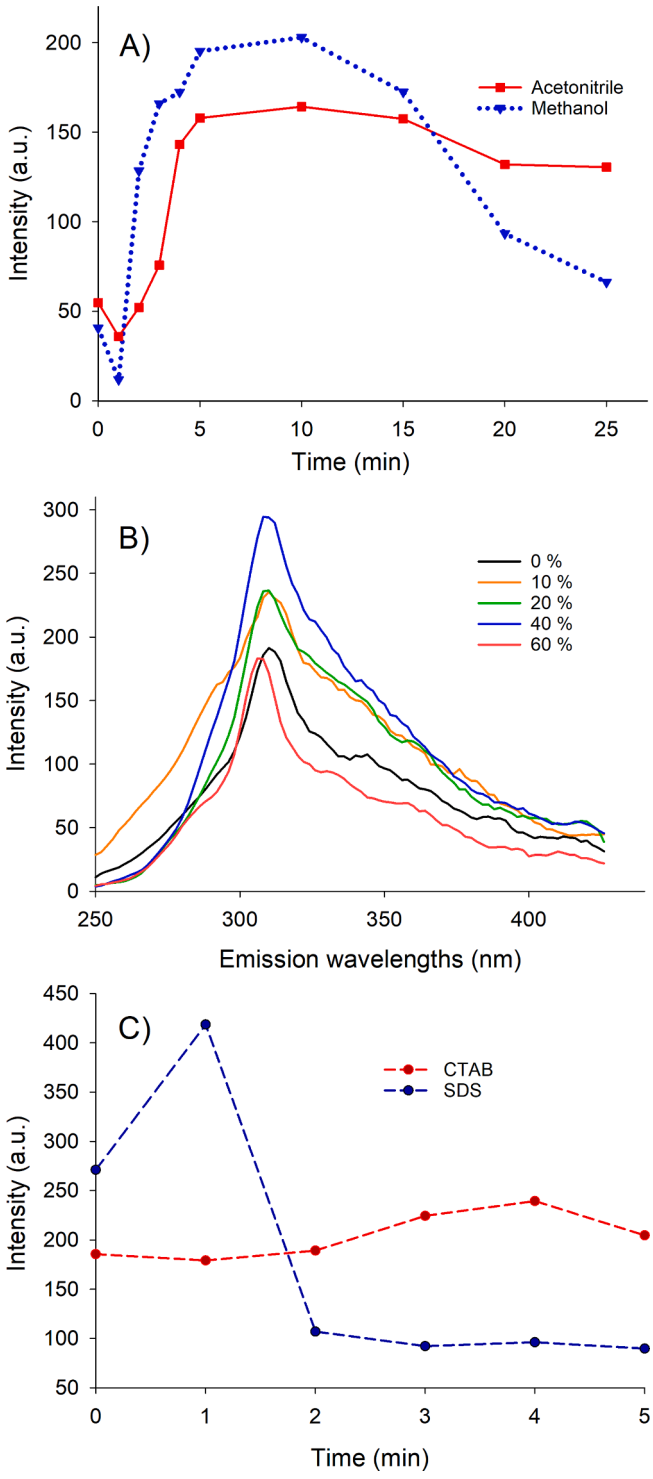

Fig. 1. Effects of experimental factors on the fluorescence response of photoproducts of deltamethrin. A) Kinetic photodegradation of deltamethrin obtained in two different organic solvents (Exc: 280 nm/Em: 314 nm). B) Emission spectra obtained in methanol with different water contents (% v/v) after 5 min of photodegradation (Exc: 280 nm). C) Kinetic photodegradation of deltamethrin obtained in methanol/water medium including different surfactants (Exc: 280 nm/Em: 314 nm).

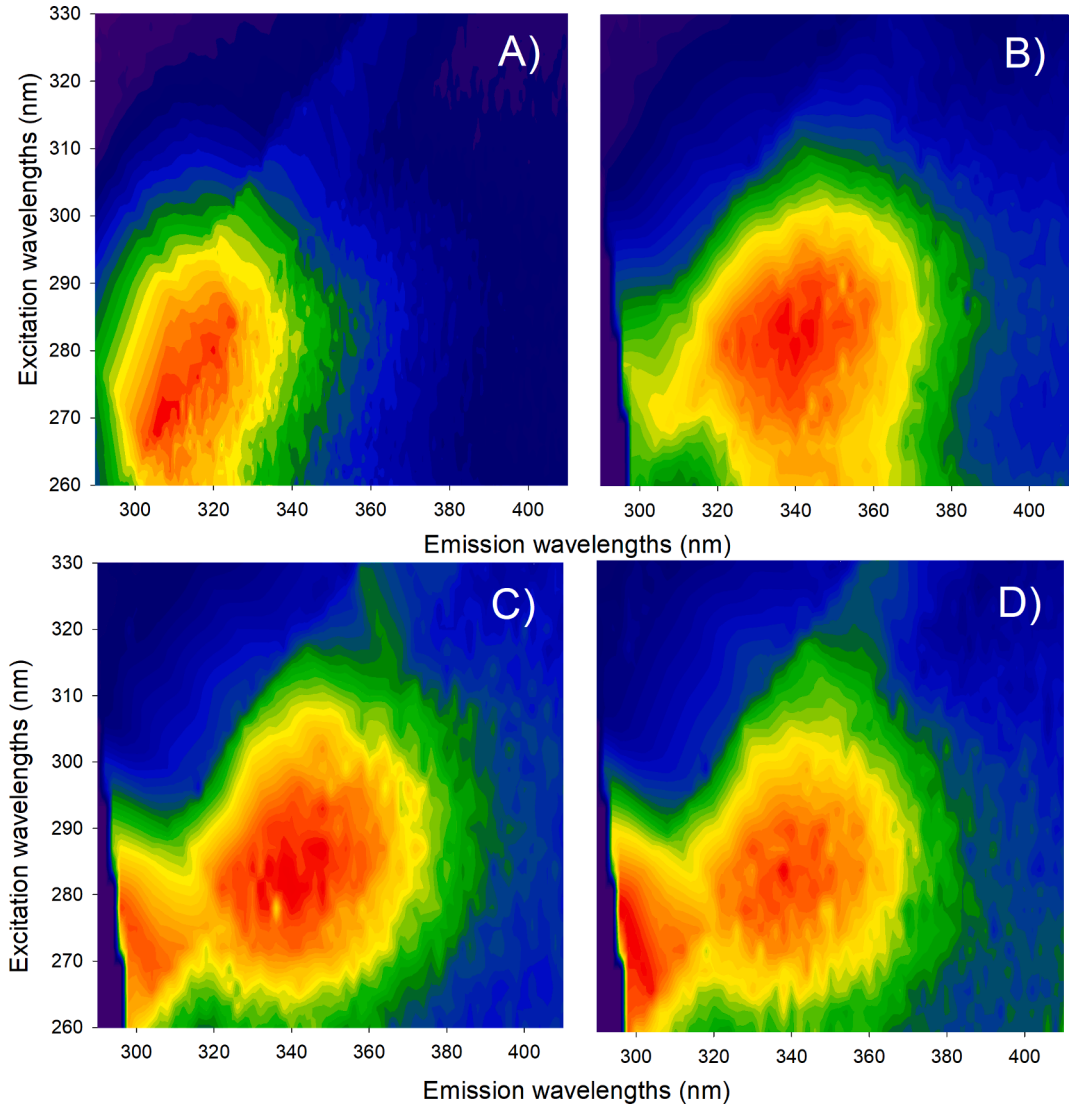

Fig. 2. Excitation-emission fluorescence matrices for deltamethrin A) without and B) with hydrogen peroxide and for the interferences C) imidacloprid and D) fipronil after 1.0 min of UV irradiation.

Then, 0.75 mL was added to a quartz cell and exposed to a UV-C lamp for degradation according to the procedure detailed in Section 3.2. All samples were analysed in duplicate.

3.5. Preconcentration for DLLME

To reach the lower limits of detection, a preconcentration method by using dispersive liquid-liquid microextraction (DLLME) was developed based on the idea proposed by Ccanccapa-Cartagena et al. [35]. After optimization of the procedure, 5.00 mL of the sample was added to a Falcon tube with 40 μL of extractant (carbon tetrachloride) and 500 μL of dispersant (acetonitrile). Then, the solution was shaken for 90 s in a vortex mixer and centrifuged for 150 s at 5000 rpm. The obtained aqueous phase was discarded, and the organic phase was evaporated at 60 °C under a stream of nitrogen until total dryness. For reconstitution, 0.3 mL of methanol and 0.2 mL of water with the same SDS and hydrogen peroxide concentrations used in the calibration were added. Finally, the same photodegradation procedure used for the standards was used for the preconcentrated water samples (see Section 3.4).

4. Results and discussion

4.1. Optimization of the fluorescence response

To obtain the best analytical performance, several experimental factors were optimized to maximize the photo-induced fluorescence response of deltamethrin. First, the effects of three different solvents (hexane, methanol and acetonitrile) on the fluorescence response and kinetic photodegradation of deltamethrin were evaluated. However, hexane was eliminated because the PIF response was lower and the occurrence of insoluble species was observed, making the fluorescence measurement difficult. Then, the PIF response at different exposition times obtained with methanol and acetonitrile was evaluated and is presented in Fig. 1A. In both solvents, a similar behaviour was observed, showing a significant increase in the photodegradation profiles within the first 5 min, followed by a decrease after 15 min. In addition, in both cases, the fluorescence decrease was observed after 1.0 min of photodegradation (the minimum observed in Fig. 1A), probably due to the formation of non-fluorescent photoproducts. However, a greater fluorescence signal and faster photodegradation kinetics were observed with methanol. Therefore, this solvent was used in further experiments.

Since the polarity of the solvent can affect the fluorescence intensity,

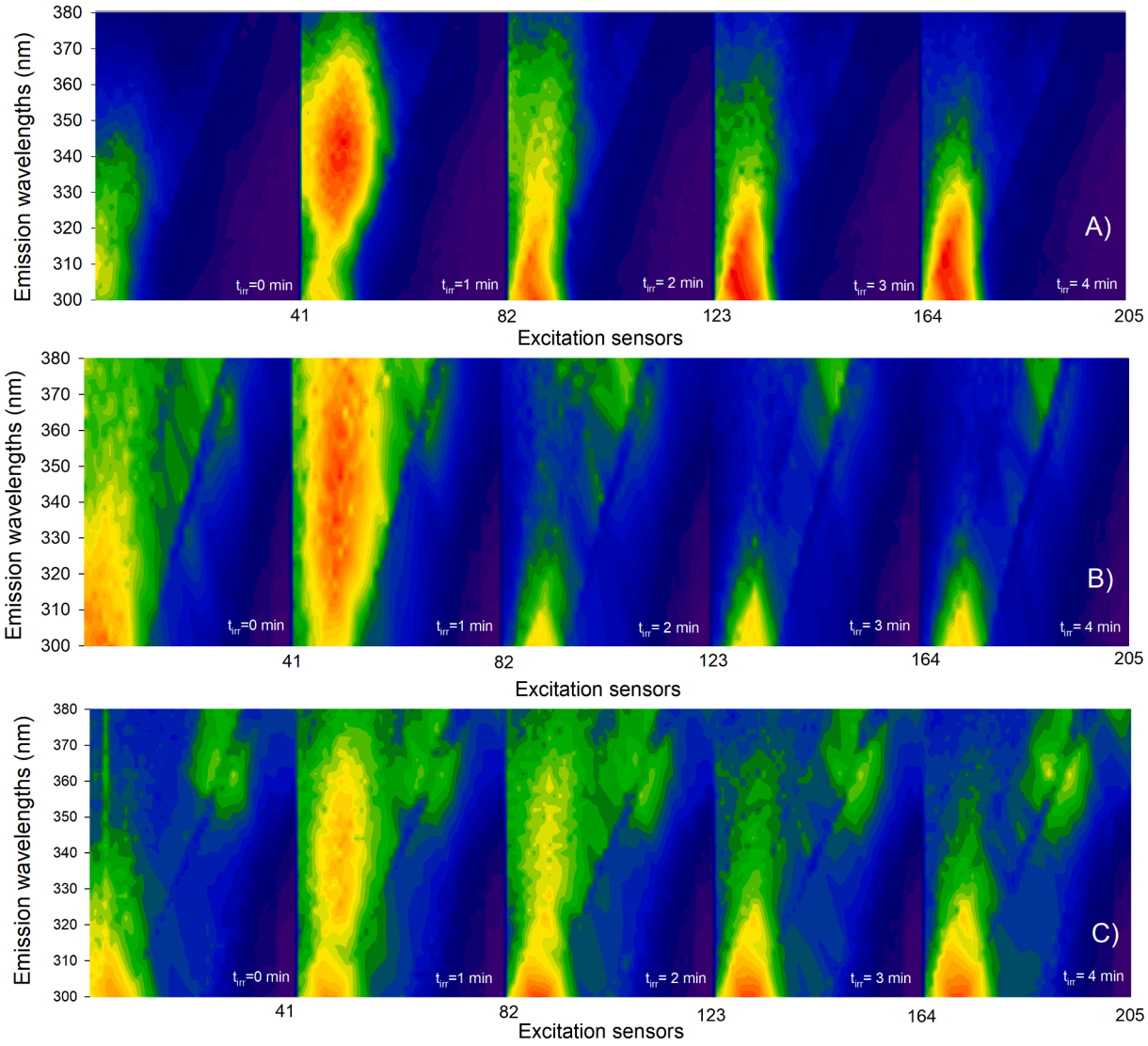

Fig. 3. Typical photodegradation kinetics followed by excitation-emission fluorescence matrices for A) the deltamethrin standard, B) a real water lagoon sample without fortification and C) an irrigation ditch sample fortified with deltamethrin to 100 μg mL^{-1}. "t_{irr}" corresponds to the time of irradiation.

the effect of the addition of different water contents on the fluorescence intensity after 5 min of photodegradation was evaluated. According to Fig. 1B, in a medium with 40% v/v water, the PIF signal of deltamethrin increased, probably due to the higher efficiency of fluorescent photoproduct formation after irradiation or the increase in the fluorescence response in this medium. Considering that changes in photophysical behaviour were not observed (e.g., the emission and excitation maxima remained at the same wavelengths), the first hypothesis appears to be more probable. Thus, 40% v/v water was adopted for subsequent experiments.

According to the literature, the addition of a surfactant can increase the fluorescence and modify the photodegradation mechanism [36]. Thus, the effects of adding cationic (CTAB) and anionic (SDS) surfactants on the PIF kinetics were evaluated. As observed in Fig. 1C, the addition of SDS dramatically reduced the fluorescent maximum (see Fig. 1A) and increased the fluorescence signal more than CTAB did. The increased fluorescence signal can be attributed to the increased rigidity of the deltamethrin photoproduct when it interacts with this surfactant [37,38], as previously reported for SDS [39]. In addition, as expected, SDS resulted in faster photodegradation than CTAB, as previously reported [40]. Therefore, SDS was used as the surfactant.

Finally, to increase the PIF response, the addition of hydrogen peroxide during photodegradation was evaluated. Previous studies reported that photosensitizers, such as hydrogen peroxide (H_2O_2), are capable of producing hydroxyl radicals that promote the photodegradation of pyrethroids [12] through an oxidation process. In this case, in the presence of H_2O_2, the PIF response increased up to 40%, while the degradation kinetics did not change, and this is similar to what is shown in Fig. 1C. In addition, as shown in Fig. 2, a redshift was observed in the fluorescence emission spectra when hydrogen peroxide was used (Fig. 2B in comparison to Fig. 2A), suggesting changes in the chemical photodegradation process due to the oxidant capacity of this photosensitizer.

In summary, the optimal media in which to evaluate the EEFM consisted of methanol with 40% water, 11 mM SDS and 5 mM H_2O_2.

4.2. Calibration and validation samples

The typical PIF kinetics followed by EEFM for one deltamethrin standard obtained under optimal conditions is presented in Fig. 3A. The maximal PIF response was observed after 1.0 min of irradiation, showing a marked decrease at higher irradiation times. In addition, other spectral signals could be observed around the PIF response of deltamethrin. These signals also appeared during blank reagent analysis

Table 1
Spectral conditions and statistical results for deltamethrin in calibration and validation samples employing EEFM data (UPLS-RBL) and EEFM-Kinetic (UPLS-RTL).

	Units	EEFM data	EEFM-Kinetic data
		UPLS-RBL model	UPLS-RTL model
Emission Wavelength	nm	290–410	290–410
Excitation wavelength	nm	290–380	290–380
PLS-Components	–	2	2
Calibration Set			
LOD	μg L^{-1}	5.3(26)[A]	0.5 (12)
LOQ	μg L^{-1}	16 (79)	1.5 (36)
Sensitivity	FU μg L^{-1}	5.6	37.6
Analytical Sensitivity	μg L^{-1}	0.6	2.2
RMSEC	μg L^{-1}	30.9	6.0
REC	%	23.7	5.5
Validation set			
LOD	μg L^{-1}	8.5 (10)	2.9 (12)
LOQ	μg L^{-1}	31 (116)	8.9 (37)
RMSEP	μg L^{-1}	45.2	12.6
REP	%	56.5	15.8

[A] : Maximum values for LOD and LOQ are presented in parenthesis. RMSEC, root mean-square error of autoprediction; REC, relative error of autoprediction; RMSEP, root mean-square error of prediction; REP, relative error of prediction; FU, fluorescence units; LOD, limit of detection; LOQ, limit of quantification. Sensitivity, analytical sensitivity, selectivity, LOD and LOQ were calculated according to Ref. [41].

and were associated with impurities in the reagents. However, an adequate multivariate model will resolve the overlap between the fluorescence response of deltamethrin and these impurities.

Preliminarily, a parallel factor analysis (PARAFAC) model was used to fit four-way data (excitation-emission-kinetic-sample modes) for the calibration set. However, no meaningful physical spectra were obtained for some of the PARAFAC components, and the core consistency was considerably low. In addition, when unmodelled interferences were present, as in the validation set or the real samples, the quality of fit decreased dramatically, probably due to high collinearity between the analyte and interferences. Similar problems have been reported previously for the PARAFAC model when high spectral collinearity or similar spectral responses were present [21,41]. Alternatively, the PARAFAC model was evaluated in the analysis of the three-way data set, arranging excitation-emission matrices after 1.0 min of irradiation. Nevertheless, the results were equally unsatisfactory. For all these reasons, this model was discarded, and only PLS variants were considered for further experiments.

The calibration set was analysed by U-PLS-RTL using a four-way array with excitation-emission-kinetic photodegradation for solutions containing only deltamethrin. The figures of merit of this model are presented in Table 1. A satisfactory data fit was attained by centring the data, adjusting the spectral window to the PIF fluorescence response and considering two PLS components. The autoprediction errors obtained for the calibration set demonstrate the GOF described. In addition, RTL components are not required for the prediction of standard concentrations. A three-way dataset was built for the calibration set, arranging the EEFMs registered for the PIF response after 1.0 min of photo-irradiation. Comparatively, the figures of merit obtained for the UPLS-RBL model suggest an inferior analytical performance. In particular, the limits of detection and quantification were considerably higher, and the analytical sensitivity was lower for the second-order model than for the third-order multivariate model. This advantage has been previously reported and was attributed to higher-order data properties [24,42]. In the same sense, the relative error of prediction (REP) was considerably lower for the third-order model, probably due to better data fitting. Similar results were obtained in previous studies, where higher-order data were used and led to improvement in the prediction error due to the best data modelling [20,23].

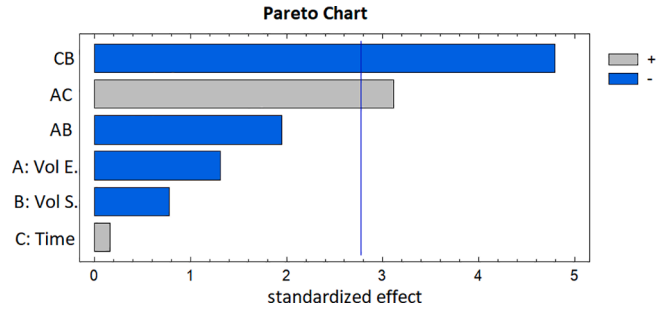

Fig. 4. Pareto chart for the studied factors in the experimental design. A: extractant volume; B: sample volume; and C: agitation time. The significant factors are higher than the error barrier (vertical blue line).

The most interesting property of multivariate models is the ability to predict the analyte concentration in the presence of unexpected interferences. For this, a validation set was prepared containing deltamethrin and two potential interferences: fipronil and imidacloprid. Fipronil belongs to the class of pesticides called phenylpyrazoles and is used to control a wide range of pests; in addition, this pesticide is bioaccumulative and does not degrade naturally [43]. On the other hand, imidacloprid belongs to the family of neonicoticoid insecticides, and this compound is widely used due to its wide range of applications [44]. Furthermore, both compounds are pesticides commonly used in agricultural applications and are potential interferences in natural waters. In addition, both compounds produce similar excitation-emission responses as deltamethrin, as evidenced in Fig. 2c and d. The results obtained during the analysis of this set of samples by UPLS-RTL are presented in Table 1. As expected, in addition to the PLS components, these samples required two RTL components for an adequate fit, and better results were obtained using the same spectral regions as those selected for the calibration set. Even when the interferences greatly overlapped in the spectral dimensions, the algorithm resolved these mixtures and quantified deltamethrin with a satisfactory relative error (15.8%). The best analytical performance of the third-order model was associated with the additional dimension with respect to the second-order model, as mentioned above. In this way, the relative error of prediction obtained with UPLS-RBL (REC: 23%; REP: 56%) was considerably higher than that obtained with UPLS-RTL, suggesting that the kinetic dimension resolved the severe overlap and collinearity present in this system. Finally, the obtained results demonstrate the superior analytical potential of using higher-order data, allowing a better fit of the data and superior figures of merit and prediction capacity.

4.3. Preconcentration of deltamethrin by DLLME

Considering the low water solubility of deltamethrin, the expected levels of this pyrethroid in natural waters are low. Therefore, a preconcentration step was evaluated for the analysis of natural water samples. To improve the analytical performance of the proposed method and incorporate green analytical approaches, a procedure based on dispersive liquid–liquid microextraction (DLLME) was evaluated in this work. Based on Ccanccapa-Cartagena et al. [35], the critical parameters considered in this method were the extractant volume (Factor A), sample volume (Factor B) and agitation duration (Factor C). The influence of these factors was studied with a two-level factorial design, including experiences at the "0″ level, (see Table S1 in the Supplementary information) using fluorescence intensity as the experimental response. The results of the experimental design are presented in the Pareto diagram shown in Fig. 4, where significant factors are higher than the error barrier (vertical blue line). This diagram indicates that the Time-Volume (CB interaction) and Extractant-Time (AC interaction) interactions have significant negative and positive effects, respectively, on the response. This result suggests that the influence of individual effects must be

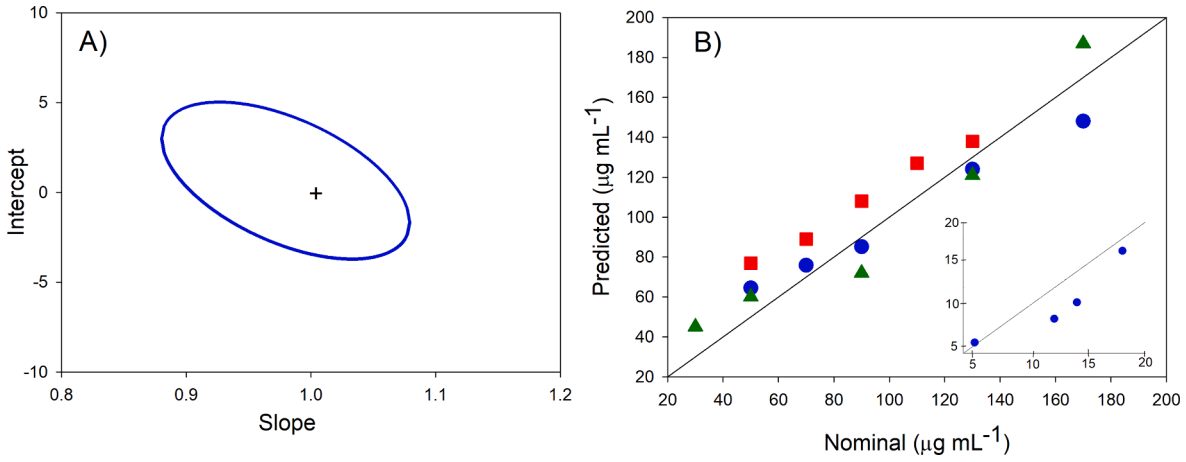

Fig. 5. (A) Elliptical joint regions (at a 95% confidence level) for the slope and intercept of the regression for fortified natural water samples. The cross marks the theoretical point (intercept: 0, slope: 1). (B) Plot of the UPLS-RTL-predicted concentrations of deltamethrin as a function of the nominal values in fortified natural water samples. Samples included the following: lagoon (filled blue circles); irrigation ditch (filled green triangles); and well water (filled red squares). Inset: Predicted concentrations of deltamethrin as a function of the nominal values in fortified natural water samples using the DLLME procedure.

considered, and the highest fluorescence response can be obtained by extracting 5000 μL of sample with 40 μL of solvent for 90 s. Under these conditions, the enrichment factors reached 10, and the limit of quantification of deltamethrin was 1.4 μg/L (as the mean) using the optimized procedure.

4.4. Real sample analysis

Natural water samples can contain dissolved organic matter, and some fluorescent compounds [45,46] can act as interferences in fluorescence detection. A typical photodegradation sequence followed by EEFM generation for some real natural water samples is presented in Fig. 3B and C. The overlap of the fluorescence response of the sample with that of deltamethrin is evident, and spectral collinearities are highly probable.

To demonstrate the ability of the method to quantify deltamethrin in natural waters, different water samples were collected and analysed. Preliminary assays showed that these samples contained deltamethrin levels lower than the detection limits. Then, a recovery study was carried out involving direct sample analysis using an external calibration method. As shown in Fig. 5A, the predicted values agree with the nominal values despite the severe spectral overlap described previously, presenting a very similar REP as that for the validation set samples (see all data in Table S2 in the Supplementary material). Similar results were observed for the preconcentrated samples (inset Fig. 5A), demonstrating the analytical capability of the proposed method.

To assess the accuracy of the predicted concentrations, the elliptical joint confidence region (EJCR) test was carried out [47]. In our case, the obtained ellipses (Fig. 5B) include the theoretically expected values of slope = 1 and intercept = 0, indicating the accuracy of predicted concentrations.

Overall, these results demonstrate the analytical capabilities of the proposed method to monitor deltamethrin levels in natural waters.

5. Conclusion

The analytical performance of the PIF response coupled to multivariate calibration was evaluated. The four-way data produced during photodegradation of deltamethrin were satisfactorily modelled by UPLS-RTL. In this complex system, especially in the presence of unexpected interferences, the four-way model showed better figures of merit and lower prediction errors due to the third-order properties. Comparison with second-order calibration suggested that these satisfactory results were associated with the additional kinetic dimension of four-way calibration, allowing us to obtain accurate results. Finally, the third-order multivariate model was satisfactorily applied to the determination of deltamethrin in natural waters despite the presence of unexpected interferents with a high overlap in both spectral dimensions. This property of higher dimensional algorithms could be highlighted as a potential third-order advantage.

CRediT authorship contribution statement

Rodrigo I. Veneciano: Methodology, Writing - original draft. **V. Sonnia Parra:** Supervision, Writing - review & editing. **Waldo Quiroz:** Funding acquisition, Writing - review & editing. **Edwar Fuentes:** Conceptualization, Writing - review & editing. **Luis F. Aguilar:** Supervision, Writing - review & editing. **Manuel A. Bravo:** Conceptualization, Writing - original draft, Funding acquisition.

Declaration of Competing Interest

The authors declare that they have no known competing financial interests or personal relationships that could have appeared to influence the work reported in this paper.

Acknowledgements

The authors acknowledge the financial support from Agencia Nacional de Investigación y Desarrollo ANID (Project Fondecyt 1190752). R. Veneciano is also grateful to the Dirección de Investigación-PUCV for the doctoral fellowship.

Appendix A. Supplementary data

Supplementary data to this article can be found online at https://doi.org/10.1016/j.microc.2020.105561.

References

[1] M. Petrarca, A. Ccanccapa, A. Masia, Comparison of green sample preparation techniques in the analysis of pyrethrins and pyrethroids in baby food by liquid chromatography – tandem mass spectrometry, J. Chromatogr. A 1497 (2017) 28–37, https://doi.org/10.1016/j.chroma.2017.03.065.
[2] W. Tang, D. Wang, J. Wang, Z. Wu, L. Li, M. Huang, S. Xu, Chemosphere Pyrethroid pesticide residues in the global environment: an overview, Chemosphere 191 (2018) 990–1007, https://doi.org/10.1016/j.chemosphere.2017.10.115.
[3] M. Koureas, A. Tsakalof, A. Tsatsakis, C. Hadjichristodoulou, Systematic review of biomonitoring studies to determine the association between exposure to

organophosphorus and pyrethroid insecticides and human health outcomes, Toxicol. Lett. 210 (2012) 155–168, https://doi.org/10.1016/j.toxlet.2011.10.007.
[4] A. Ma, Research progress on analytical technique of pyrethroid pesticide residue, J. Anhui Agric. Sci. 37 (2009) 13775–13777.
[5] A.M. Saillenfait, D. Ndiaye, J.P. Sabaté, Pyrethroids: exposure and health effects – an update, Int. J. Hyg. Environ. Health 218 (2015) 281–292, https://doi.org/10.1016/j.ijheh.2015.01.002.
[6] Z.M. Chen, Y.H. Wang, Chromatographic methods for the determination of pyrethrin and pyrethroid pesticide residues in crops, foods and environmental samples, J. Chromatogr. A 754 (1996) 367–395, https://doi.org/10.1016/S0021-9673(96)00490-6.
[7] P.P. Vázquez, A.R. Mughari, M.M. Galera, Application of solid-phase microextraction for determination of pyrethroids in groundwater using liquid chromatography with post-column photochemically induced fluorimetry derivatization and fluorescence detection, J. Chromatogr. A 1188 (2008) 61–68, https://doi.org/10.1016/j.chroma.2008.02.030.
[8] E.M. Kristenson, S. Shahmiri, C.J. Slooten, R.J.J. Vreuls, U.A.T. Brinkman, Matrix solid-phase dispersion micro-extraction of pesticides from single insects with subsequent GC-MS analysis, Chromatographia 59 (2004) 315–320, https://doi.org/10.1365/s10337-003-0166-8.
[9] A. Venant, E. Van Neste, S. Borrel, J. Mallet, Determination of residues of deltamethrin in milk and butter, Food Addit. Contam. 7 (1990) 117–123, https://doi.org/10.1080/02652039009373828.
[10] W.G. Taylor, D.D. Vedres, T.W. Hall, Capillary gas chromatographic determination of permethrin insecticide by transesterification, J. Chromatogr. B Biomed. Appl. 690 (1997) 123–129, https://doi.org/10.1016/S0378-4347(96)00367-2.
[11] J. Mao, K.M. Erstfeld, P.H. Fackler, Simultaneous determination of tralomethrin, deltamethrin, and related compounds by HPLC with radiometric detection, J. Agric. Food Chem. 41 (1993) 596–601, https://doi.org/10.1021/jf00028a017.
[12] P. Liu, Y. Liu, Q. Liu, J. Liu, Photodegradation mechanism of deltamethrin and fenvalerate, J. Environ. Sci. 22 (2010) 1123–1128, https://doi.org/10.1016/S1001-0742(09)60227-8.
[13] R. Adamou, A. Coly, A. Abdoulaye, M. Soumaila, I. Moussa, K. Ikhiri, A. Tine, Photochemically-induced fluorescence dosage of non-fluorescent pyrethroid (etofenprox) in natural water using a cationic micellar medium, J. Fluoresc. 21 (2011) 1409–1415, https://doi.org/10.1007/s10895-010-0824-9.
[14] A. Coly, J.J. Aaron, Cyclodextrin-enhanced fluorescence and photochemically-induced fluorescence determination of five aromatic pesticides in water, Anal. Chim. Acta 360 (1998) 129–141, https://doi.org/10.1016/S0003-2670(97)00721-6.
[15] A. Coly, J.J. Aaron, Fluorimetric analysis of pesticides: Methods, recent developments and applications, Talanta 46 (1998) 815–843, https://doi.org/10.1016/S0039-9140(97)00366-4.
[16] A. Garrido Frenich, M. Martínez Galera, J.L. Martínez Vidal, M.D. Gil García, Partial least-squares and principal component regression of multi-analyte high-performance liquid chromatography with diode-array detection, J. Chromatogr. A 727 (1996) 27–38, https://doi.org/10.1016/0021-9673(95)01150-1.
[17] Y.Y. Yuan, S.T. Wang, S.Y. Liu, Q. Cheng, Z.F. Wang, D.M. Kong, Green approach for simultaneous determination of multi-pesticide residue in environmental water samples using excitation-emission matrix fluorescence and multivariate calibration, Spectrochim. Acta Part A 228 (2020), 117801, https://doi.org/10.1016/j.saa.2019.117801.
[18] X.D. Sun, H.L. Wu, Y. Chen, J.C. Chen, R.Q. Yu, Chemometrics-assisted calibration transfer strategy for determination of three agrochemicals in environmental samples: solving signal variation and maintaining second-order advantage, Chemom. Intell. Lab. Syst. 194 (2019), 103869, https://doi.org/10.1016/j.chemolab.2019.103869.
[19] V.D. Singh, S.J. Daharwal, Development and validation of multivariate calibration methods for simultaneous estimation of Paracetamol, Enalapril maleate and hydrochlorothiazide in pharmaceutical dosage form, Spectrochim. Acta Part A 171 (2017) 369–375, https://doi.org/10.1016/j.saa.2016.08.028.
[20] A.C. Olivieri, G.M. Escandar, Analytical chemistry assisted by multi-way calibration: a contribution to green chemistry, Talanta 204 (2019) 700–712, https://doi.org/10.1016/j.talanta.2019.06.022.
[21] A. Osorio, C. Toledo-Neira, M.A. Bravo, Critical evaluation of third-order advantage with highly overlapped spectral signals. Determination of fluoroquinolones in fish-farming waters by fluorescence spectroscopy coupled to multivariate calibration, Talanta 204 (2019) 438–445, https://doi.org/10.1016/j.talanta.2019.06.048.
[22] X.H. Zhang, X.D. Qing, H.L. Wu, Discussion on the superiority of third-order advantage: analytical application for four-way data in complex system, Microchem. J. 145 (2019) 1078–1085, https://doi.org/10.1016/j.microc.2018.12.037.
[23] X.H. Zhang, H.L. Wu, X.L. Yin, Y. Li, X.D. Qing, H.W. Gu, C. Kang, R.Q. Yu, Exploiting third-order advantage using four-way calibration method for direct quantitative analysis of active ingredients of Schisandra chinensis in DMEM by processing four-way excitation-emission-solvent fluorescence data, Chemom. Intell. Lab. Syst. 155 (2016) 46–53, https://doi.org/10.1016/j.chemolab.2016.04.008.
[24] M.R. Alcaraz, O. Monago-Maraña, H.C. Goicoechea, A. Muñoz de la Peña, Four- and five-way excitation-emission luminescence-based data acquisition and modeling for analytical applications. A review, Anal. Chim. Acta 1083 (2019) 41–57.
[25] M.D. Carabajal, J.A. Arancibia, G.M. Escandar, Multivariate curve resolution strategy for non-quadrilinear type 4 third-order/four way liquid chromatography–excitation-emission fluorescence matrix data, Talanta 189 (2018) 509–516, https://doi.org/10.1016/j.talanta.2018.07.017.
[26] E. Fuentes, C. Cid, M.E. Báez, Determination of imidacloprid in water samples via photochemically induced fluorescence and second-order multivariate calibration, Talanta 134 (2015) 8–15, https://doi.org/10.1016/j.talanta.2014.11.017.
[27] A.C. Olivieri, On a versatile second-order multivariate calibration method based on partial least-squares and residual bilinearization: Second-order advantage and precision properties, J. Chemom. 19 (2005) 253–265, https://doi.org/10.1002/cem.927.
[28] S. Wold, P. Geladi, K. Esbensen, J. Öhman, Multi-way principal components-and PLS-analysis, J. Chemom. 1 (1987) 41–56, https://doi.org/10.1002/cem.1180010107.
[29] S.A. Bortolato, J.A. Arancibia, G.M. Escandar, Chemometrics-assisted excitation-emission fluorescence spectroscopy on nylon membranes. Simultaneous determination of benzo[a]pyrene and dibenz[a, h]anthracene at parts-per-trillion levels in the presence of the remaining EPA PAH priority pollutants as int, Anal. Chem. 80 (2008) 8276–8286, https://doi.org/10.1021/ac801458a.
[30] J.A. Arancibia, A.C. Olivieri, D.B. Gil, A.E. Mansilla, I. Durán-Merás, A.M. De La Peña, Trilinear least-squares and unfolded-PLS coupled to residual trilinearization: new chemometric tools for the analysis of four-way instrumental data, Chemom. Intell. Lab. Syst. 80 (2006) 77–86, https://doi.org/10.1016/j.chemolab.2005.08.002.
[31] A. Jiménez Girón, I. Durán-Merás, A. Espinosa-Mansilla, A. Muñoz de la Peña, F. Cañada Cañada, A.C. Olivieri, On line photochemically induced excitation-emission-kinetic four-way data. Analytical application for the determination of folic acid and its two main metabolites in serum by U-PLS and N-PLS/residual trilinearization (RTL) calibration, Anal. Chim. Acta 622 (2008) 94–103, https://doi.org/10.1016/j.aca.2008.05.079.
[32] R. Zepp, W. Sheldon, M.A. Moran, Dissolved organic fluorophores in southeastern US coastal waters: correction method for eliminating Rayleigh and Raman scattering peaks in excitation-emission matrices, Mar. Chem. 89 (2004) 15–36, https://doi.org/10.1016/j.marchem.2004.02.006.
[33] A.C. Olivieri, H.L. Wu, R.Q. Yu, MVC2: a MATLAB graphical interface toolbox for second-order multivariate calibration, Chemom. Intell. Lab. Syst. 96 (2009) 246–251, https://doi.org/10.1016/j.chemolab.2009.02.005.
[34] S.J. Mazivila, S.A. Bortolato, A.C. Olivieri, MVC3_GUI: a MATLAB graphical user interface for third-order multivariate calibration. An upgrade including new multi-way models, Chemom. Intell. Lab. Syst. 173 (2018) 21–29, https://doi.org/10.1016/j.chemolab.2017.12.012.
[35] A. Ccanccapa-Cartagena, A. Masiá, Y. Picó, Simultaneous determination of pyrethroids and pyrethrins by dispersive liquid-liquid microextraction and liquid chromatography triple quadrupole mass spectrometry in environmental samples, Anal. Bioanal. Chem. 409 (2017) 4787–4799, https://doi.org/10.1007/s00216-017-0422-7.
[36] M.C. Icardo, J.M. Calatayud, Photo-induced luminescence, Crit. Rev. Anal. Chem. 38 (2008) 118–130, https://doi.org/10.1080/10408340802039609.
[37] H. Singh, W.L. Hinze, Micellar enhanced spectrofluorimetric methods: application to the determination of pyrene, Anal. Lett. 15 (1982) 221–243, https://doi.org/10.1080/00032718208064379.
[38] A. Coly, J.J. Aaron, Photochemically-induced fluorescence determination of sulfonylurea herbicides using micellar media, Talanta 49 (1999) 107–117, https://doi.org/10.1016/S0039-9140(98)00349-X.
[39] J.J. Aaron, A. Coly, Photochemical-spectrofluorimetric determination of two pyrethroid insecticides using an anionic micellar medium, Analyst 121 (1996) 1545–1549, https://doi.org/10.1039/AN9962101545.
[40] A.M. García-Campaña, J.J. Aaron, J.M. Bosque-Sendra, Micellar-enhanced photochemically induced fluorescence detection of chlorophenoxyacid herbicides. Flow injection analysis of mecoprop and 2,4-dichlorophenoxyacetic acid, Talanta 55 (2001) 531–539, https://doi.org/10.1016/S0039-9140(01)00470-2.
[41] M. Bravo, L.F. Aguilar, W. Quiroz, A.C. Olivieri, G.M. Escandar, Determination of tributyltin at parts-per-trillion levels in natural waters by second-order multivariate calibration and fluorescence spectroscopy, Microchem. J. 106 (2013) 95–101.
[42] A.C. Olivieri, Analytical figures of merit: from univariate to multiway calibration, Chem. Rev. 114 (2014) 5358–5378, https://doi.org/10.1021/cr400455s.
[43] R.C. Gupta, A. Anadón, Chapter 42 – Fipronil, in: R.C.B.T.-V.T. Third E. Gupta (Ed.), Academic Press, 2018: pp. 533–538. doi:10.1016/B978-0-12-811410-0.00042-8.
[44] L.P. Sheets, Chapter 95 – Imidacloprid: A Neonicotinoid Insecticide, in: R.B.T.-H.H. of P.T. Third E. Krieger (Ed.), Academic Press, New York, 2010: pp. 2055–2064. doi:10.1016/B978-0-12-374367-1.00095-1.
[45] N. Hudson, A. Baker, D. Reynolds, Fluorescence analysis of dissolved organic matter in natural, waste and polluted waters – a review, River Res. Appl. 23 (2007) 631–649, https://doi.org/10.1002/rra.1005.
[46] R. Del Vecchio, N. Blough, Photobleaching of chromophoric dissolved organic matter in natural waters: kinetics and modeling, Mar. Chem. 78 (2002) 231–253, https://doi.org/10.1016/S0304-4203(02)00036-1.
[47] A.G. González, M.A. Herrador, A.G. Asuero, Intra-laboratory testing of method accuracy from recovery assays, Talanta 48 (1999) 729–736, https://doi.org/10.1016/S0039-9140(98)00271-9.